A ΔΣM-Based Reconfigurable Direct-Digitization AFE for ECG, BioZ, PPG, and GSR in Wearables

Chenxi Wang, Yuxiang Tang, Xiuzhi Zhao, Xianglong Chen, Tianxiang Qu, Zhiliang Hong, and Jiawei Xu
State Key Laboratory of Integrated Chips and Systems, Fudan University, Shanghai, China.
Email: jwxu@fudan.edu.cn

***Abstract*—This paper presents a reconfigurable direct-digitization analog front-end circuit (DD-AFE) for multimodal physiological signal acquisition, supporting ECG, BioZ, PPG, and GSR in a single AFE. The architecture leverages a second-order ΔΣ modulator featuring a reconfigurable integrator and reusable auxiliary circuits for voltage or current excitation, DC cancellation, and LED driving, improving circuit utilization across sensing modalities. Fabricated in 0.18-μm CMOS, the proposed DD-AFE occupies 1.56 mm². With chopping and linearity enhancement techniques, it achieves a peak SNDR of 97.7 dB and a dynamic range (DR) of 108.2 dB over a 500-Hz bandwidth, while maintaining an input impedance exceeding 1.6 GΩ at 50 Hz. In BioZ mode, the AFE achieves a maximum SNR of 96.6 dB. In PPG and GSR modes, the input-referred current noise is 2.1 pA_{rms} within a 4-Hz bandwidth. This work is the first ΔΣM-based reconfigurable DD-AFE that integrates the acquisition of four major physiological signal types, while delivering competitive noise, linearity, and energy efficiency compared with state-of-the-art single-modality AFEs.**

Keywords*—Reconfigurable, analog front-end, ΔΣM, direct-digitization, multimodal, physiological signal acquisition, ECG, bioimpedance, PPG, GSR.

I. Introduction

Wearable devices integrating multiple sensors, including wrist-worn devices, epidermal patches, smart garments, and rings, have emerged as a key hardware platform for daily health monitoring and edge AI-enabled healthcare [1]. These systems support a wide range of applications including cardiovascular and blood pressure monitoring, sleep and respiratory analysis, stress and emotional state assessment, and fitness tracking. Such applications impose stringent design constraints on the analog front-end (AFE), demanding compact area for wearability, low power for extended battery life, and wide dynamic range (DR) for reliable physiological signal acquisition [2]. Consequently, single-chip multimodal AFEs capable of acquiring ECG, PPG, BioZ, and GSR have attracted significant interest, as they enable the measurement of voltage, current, impedance, and conductance within a unified sensing interface (Fig. 1).

Existing multimodal AFEs can be broadly classified into parallel and reconfigurable architectures. Parallel AFEs (Fig. 2a) [2][3] enable simultaneous multi-channel acquisition, but their area and power consumption scale linearly with channel count, limiting scalability and power efficiency. On the other hand, reconfigurable AFEs improve hardware utilization and can be further divided into IA+ADC architectures (Fig. 2b) [4][5] and ΔΣM-based direct-digitization AFEs (DD-AFEs) (Fig. 2c) [6][7]. IA+ADC architectures suffer from intrinsic limitations in DR and linearity due to separation of analog amplification and quantization stages. ΔΣM-based DD-AFEs offer higher precision by integrating signal conditioning and digitization. Nevertheless, prior reconfigurable ΔΣM-based implementations remain constrained in noise and linearity, and lack dedicated excitation or bias for other physiological

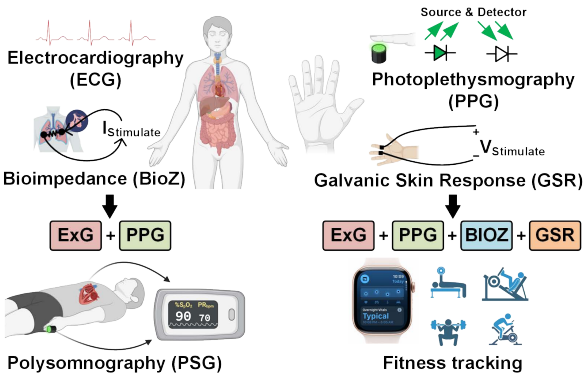

Fig. 1. Multi-modal physiological signal acquisition requirements

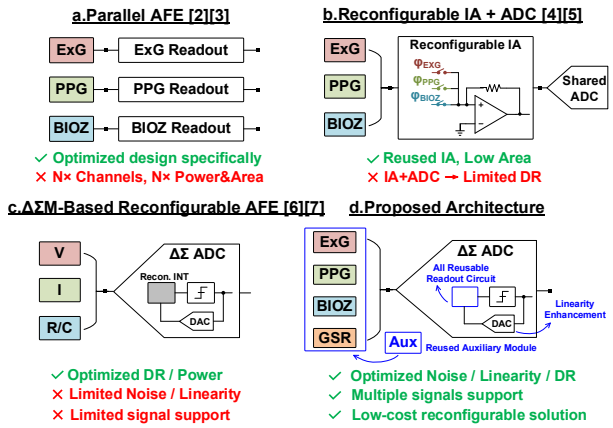

Fig. 2. Prior work and proposed architecture

modalities such as PPG and BioZ, thereby limiting their uses in fully integrated multimodal sensing systems.

To address these limitations, this work proposes a ΔΣM-based reconfigurable DD-AFE architecture, as illustrated in Fig. 2d. By low-cost reconfiguration of the first integrator stage, the readout (RO) section achieves full hardware reuse while optimizing noise and linearity, thereby overcoming the DR and precision limitations of prior IA+ADC architectures. In addition, a reusable auxiliary circuit supporting both current and voltage excitation enables efficient acquisition of diverse physiological modalities without duplicating dedicated front-end blocks. As a result, the proposed DD-AFE architecture reduces area overhead compared to parallel AFEs, while still achieving a DR exceeding 100 dB and linearity above 95 dB across multiple operating modes.

II. System Architecture

Fig. 3 shows the proposed architecture of reconfigurable DD-AFE, comprising a readout path and an auxiliary support block. The readout path adopts a second-order ΔΣ modulator, with reconfigurability realized at the degeneration resistor R_{INT1} of input transconductor (G_{m1}). By configuring switches to select either a resistor or different sensing elements, such

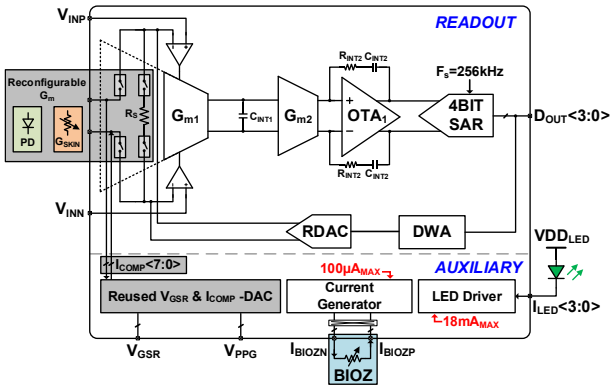

Fig. 3 Proposed reconfigurable Δ-Σ based AFE

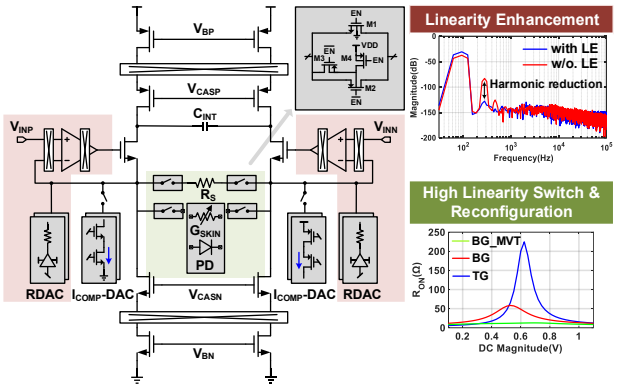

Fig. 4 Proposed reconfigurable input G_{m1} stage and simulation results

as photodiodes and skin-conductance electrodes, at this node, the unified architecture converts heterogeneous physiological signals into balanced differential currents for ΔΣ digitization.

The auxiliary block in Fig.3 provides modality-dependent excitation and biasing, while also reusing several functional modules across sensing modes. A programmable DC voltage source provides an adjustable DC level for GSR body bias or photodiode bias in PPG operation. In both PPG and GSR modes, this voltage source is also partially reused in a current DAC (I_{COMP}-DAC) that cancels the baseline input DC current. In contrast, the current excitation module for BioZ sensing and the LED driver for PPG illumination are not reused, as their noise budgets and amplitude ranges differ significantly across modes.

Fig. 4 illustrates the implementation of the reconfigurable input stage. A gain-boosted source follower together with the series degeneration resistor (R_S = 50 kΩ) establishes a nearly constant integrator transconductance G_{m1}, thereby improving linearity. At the reconfiguration node (highlighted in green), variations in the switch on-resistance affect the degeneration resistance and degrade linearity. To mitigate this effect, low-R_{on} body-grabbing (BG) switches [4] are used. Implemented with medium-V_{TH} devices, the BG switches reduce R_{on} from 200 Ω to 10 Ω, making its contribution negligible compared with the 50-kΩ degeneration resistor and thereby preserving integrator linearity. In PPG or GSR modes, the degeneration resistor can be replaced by external sensing elements such as a photodiode (PD) or GSR electrodes.

A. ECG Mode

Fig. 5 illustrates the circuit configuration under different operating modes. In ECG mode, the feedback current of the R-DAC is applied across R_S, enabling high linearity with a

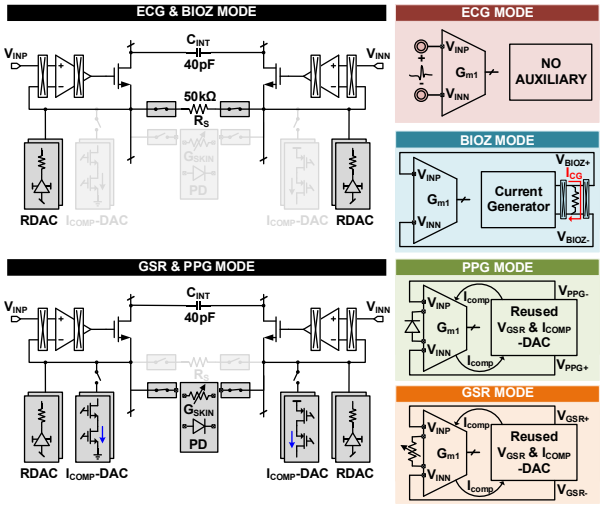

Fig. 5 Configuration scheme for multimodal measurement

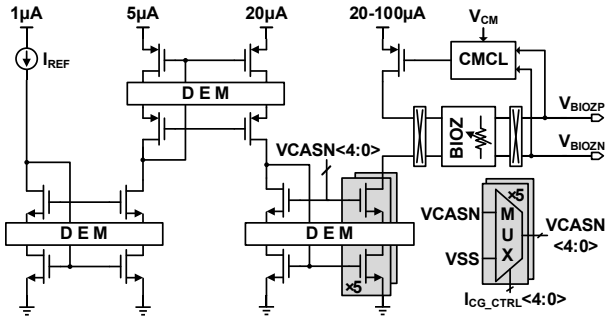

Fig. 6 The BioZ current generator (CG)

reduced bias current of 1.5 μA. The embedded chopping [8] mitigates flicker noise while achieving high input impedance, enabling dry-electrode ECG acquisition. The G_{m1} differential inputs are directly connected to the body through electrodes, while the body bias is supplied by an external reference.

B. BioZ Mode

As shown in Fig. 5 (top right), the BioZ mode employs a current generator (CG) to produce an AC stimulus I_{CG} at 64 kHz. The injected current flows through the body impedance, generating a differential voltage V_{BIOZ} that is processed by the input G_{m1}. Fig. 6 shows a simplified schematic of the CG. The 20-100 μA output current is generated from I_{REF} = 1 μA and scaled through current mirrors, with a cascoded structure and dynamic element matching (DEM) to improve current accuracy and mitigate 1/*f* noise.

A common-mode control loop (CMCL) [9] regulates CM voltage fluctuations. Functionally similar to CMFB, the loop senses the CM component of V_{BIOZ}, compares it with a target reference V_{CM}, and adjusts the PMOS current source. This CG architecture eliminates the complementary branch of the PMOS current mirror, considerably reducing power and area while stabilizing the input CM voltage for G_{m1}.

C. PPG Mode

In PPG mode (Fig. 5 lower left), The PD is connected to G_{m1} with the compensation current path I_{COMP} enabled. The auxiliary amplifier within G_{m1} applies the bias across the PD terminals, reducing the effective parasitic capacitance C_{PD}.

Fig. 7 shows a simplified schematic of the reusable DAC for DC current compensation in PPG mode and for GSR bias. Unit resistors in the reference-current generation are matched

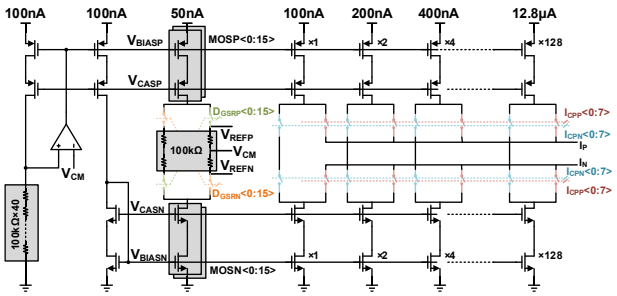

Fig. 7 The reused V_{GSR} and I_{COMP} DAC

to those in the voltage-generation path to guarantee accuracy. An on-chip binary-to-thermometer decoder controls voltage excitation and current compensation via thermometer-coded signals. The voltage excitation is programmable from V_{CM} ± 5mV to V_{CM} ± 75mV in 5 mV steps, and the compensation current spans from 100 nA to 25.6 μA.

An integrated LED driver provides optical excitation in constant-current mode. Operating in constant-current mode, with a programmable drive current from 1.2 mA to 18 mA in 1.2 mA steps.

D. GSR Mode

In GSR mode, a DC bias applied across the skin produces a current proportional to the skin conductance G_{SKIN}, whose variations are sensed by the DD-AFE. GSR measurement is challenging due to the wide DR of G_{SKIN} and the large DC component. The circuit configuration is similar to that of the PPG mode. A fully differential structure improves CMRR and suppresses supply disturbances. This design employs the reusable IDAC to compensate for the DC component, while the programmable DAC bias together with the ΔΣM readout accommodates the wide conductance range. Furthermore, the DAC is fully reused, enabling efficient hardware sharing.

III. Measurement Results

The DD-AFE is fabricated in a 0.18-μm CMOS process and operates from a 1.2 V supply. The core area is 1.3 mm × 1.2 mm, with the reconfigurable readout circuit occupying 0.75 mm² (Fig. 8, left). Fig. 8 (right) summarizes the power consumption for the four modes. All modes except ECG include auxiliary programmable-current module, resulting in configuration-dependent power.

Fig. 9 shows the performance of the DD-AFE configured in ECG mode. Operating at a 256 kHz sampling frequency with an OSR of 256, the DD-AFE achieves a peak SNDR of 97.7 dB and an SNR of 103.1 dB over a 500 Hz bandwidth. Enabling chopping improves the SNR by 7.3 dB. The input noise density is 63.8 nV/√Hz, remaining nearly flat at low-frequencies. Due to the low noise floor, the readout achieves a DR of 108.2 dB and supports a maximum input amplitude exceeding 350mV_{pp}, ensuring robust ECG signals acquisition. The input impedance is 44 GΩ at 10 Hz and 1.6 GΩ at 50 Hz, mitigating signal attenuation and measurement errors caused by the finite impedance at the electrode-tissue interface.

Fig. 10 presents the measured noise performance in the BioZ, PPG/GSR modes. In BioZ mode, measurements using I_{CG} and a sense resistor yield the equivalent impedance noise and SNR over a 0.1-4 Hz bandwidth, with a maximum SNR of 96.6 dB. In GSR and PPG modes, a 500 kΩ resistor (≈ 2 μS) is connected as the input load, with a ±50 mV excitation voltage applied. With DC-compensation IDAC and chopping enabled, the integrated input-referred current noise 2.1 pA_{rms} (BW=4Hz). Compared with the non-chopped case, 1/*f* noise

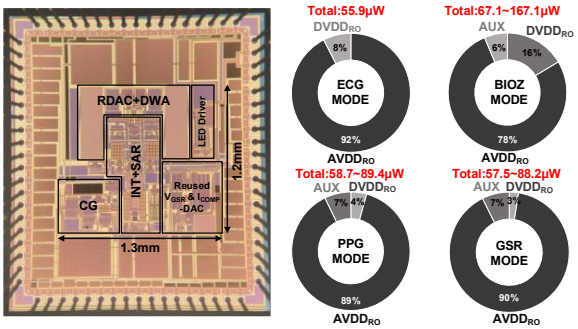

Fig. 8 Die photo and power breakdown

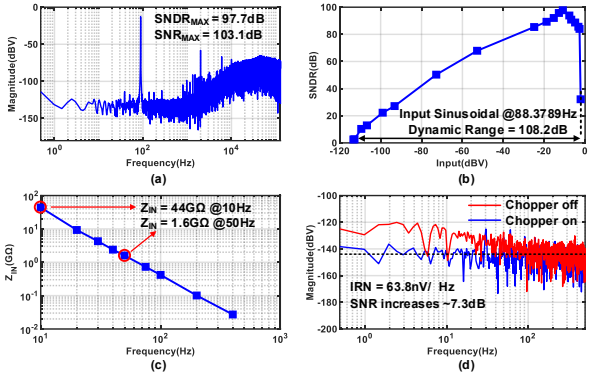

Fig. 9 Performance of the DD-AFE in ECG mode

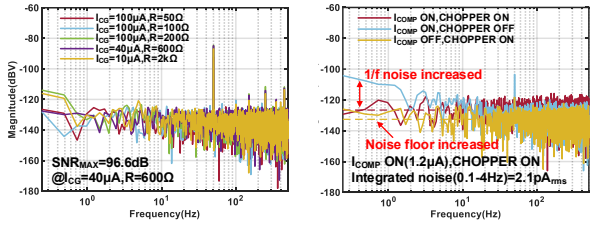

Fig. 10 Noise performance of BioZ mode (left), PPG and GSR modes (right)

is reduced by 83.6%, while the IDAC contributes half of the total noise.

Fig. 11 presents the measurement setup for physiological signal acquisition For ECG and BioZ, surface electrodes are positioned at the corresponding anatomical locations. In PPG mode, the LED is placed in contact with the fingertip or wrist. GSR mode is evaluated using two finger-worn sleeves, with each integrating an electrode.

Fig. 12 shows the measurement results. In ECG and PPG modes, the acquired waveforms effectively reflect heart rate variability. In BioZ mode, the impedance variations clearly distinguish shallow breathing from breath holding. In GSR mode, the skin conductance signals reveal autonomic activity associated with shallow and deep breathing.

Table II compares the proposed work with state-of-the-art multimodal physiological signal acquisition ICs. Among ΔΣM-based reconfigurable DD-AFEs, the proposed design is the first to support ECG, PPG, BioZ, and GSR acquisition within a unified readout architecture. Functionally, it enables comprehensive sensing across the four fundamental domains: voltage (V), current (I), resistance (R), and conductance (G). To reduce cost, the design integrates four modalities within a compact structure, minimizing area and hardware complexity. Performance-wise, it demonstrates low noise, wide DR, and the highest reported FoM_{DR} among comparable designs.

TABLE I. COMPARISON WITH STATE-OF-THE-ART

	VLSIC17 [4]	ASSCC24 [5]	ISSCC19 [2]	ISSCC24 [3]	ISSCC24 [6]	ISCAS24 [7]	This work
Architecture	**Reconfigurable IA + ADC**		**Parallel IA + ADC**		**ΔΣ-based Reconfigurable DD-AFE**		
Process (nm)	180	55	55	180	180	180	180
Sensing Modality	ECG/BioZ/GSR /GPA/PPG	ECG/PPG /BioZ	ECG/PPG /BioZ	Chemical/ECG/ PPG/BioZ	V/I	V/I/C	ECG/PPG /BioZ/GSR
Area (mm^2)	1.18[a]	1.8	4.79[a]	6.6	0.32	1.17[d]	**0.75/1.56[b]**
ECG Mode (V Sensing)							
Power (μW)	33	35	40	72	13.5	22.2	55.9
IRN ($μV_{rms}$)@BW	0.8@100Hz	8.3@2kHz	0.81@150Hz	0.27@125Hz	12@10kHz	N/A@2kHz	**0.78@150Hz**
Z_{IN} (Ω)	140M@50Hz	400M@N/A	>500M@50Hz	N/A	300M@DC	N/A	**1.6G@50Hz**
PPG or GSR Mode (I Sensing)							
Power (μW)	20	N/A	121	155	13.5	37.7	58.7
IRN (pA_{rms})@BW	82@4Hz	18@10Hz	28@20Hz	N/A	78.4@5kHz	N/A	**2.1@4Hz**
DR (dB)	N/A	>60	94/111[c]	108[c]	114[c]	60	108/146[c]
BioZ Mode (R or C Sensing)							
Power (μW)	36	45	74	12.8	N/A	23	67.1
Noise (mΩ/√Hz)	10	90	3	N/A	N/A	N/A	**1.38**
DR (dB)	N/A	80	N/A	145.2[c]	N/A	97.8	>100
ADC Only							
SNDR (dB)	64.37[d]	N/A	78.82[d]	74/110.12	85(V)/76(I)	57(V)/54(I)/75(C)	**97.7**
FoM_{DR}[e]	167.29[d]	N/A	N/A	N/A	175[a]	168.2	**177.72**

[a] estimated; [b] readout / readout + auxiliary circuits; [c] DR with DC extension; [d] based on calculation; [e] only compare single ADC structure, no DC extension

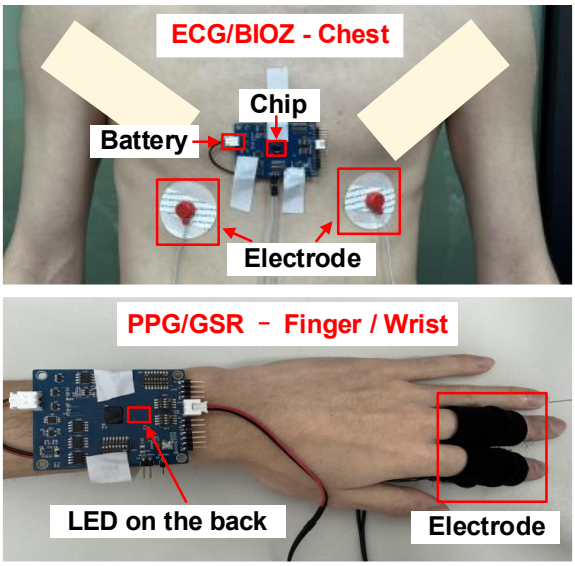

Fig. 11 Measurement setup

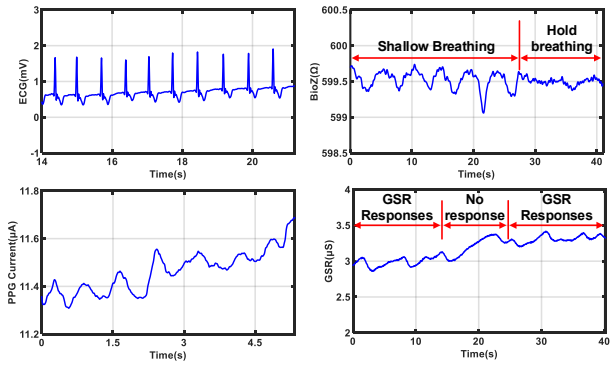

Fig. 12 Multimodal physiological signal measurements

Relative to reconfigurable IA+ADC architectures, the proposed design achieves higher SNDR and DR. Thanks to the closed-loop ΔΣM that improves linearity and mitigates noise at comparable power and area. Compared to parallel AFE implementations, it achieves reduced area and power consumption while preserving competitive accuracy across all configurable modes.

IV. CONCLUSION

To address the area, power, and flexibility limitations of parallel AFEs, this work proposes a reconfigurable DD-AFE architecture. Leveraging a reusable ΔΣM architecture and auxiliary circuits, the design acquires four fundamental physiological signals with high precision, wide dynamic range, and superior energy efficiency across four operating modes, ensuring accurate and reliable sensing in wearables.

ACKNOWLEDGMENT

This work was supported by National Natural Science Foundation of China (Grant No. 62474046).

REFERENCES

[1] Y. Suo, H. Guo, R. Yu and Y. Zhao, "Wearable Sensors for Vital Signs: A Review of 20 Years and Future Directions," *Integrated Circuits and Systems*, vol. 1, no. 4, pp. 215-226, Sept.-Oct. 2024

[2] M. Konijnenburg et al., "A 769μW Battery-Powered Single-Chip SoC With BLE for Multi-Modal Vital Sign Health Patches," *ISSCC*, pp. 360-362, Feb, 2019

[3] J. Cho et al., "An Adhesive Interposer-Based Reconfigurable Multi-Sensor Patch Interface with On-Chip Application Tunable Time-Domain Feature Extraction," *ISSCC*, pp. 554-556, Feb. 2024.

[4] J. Xu et al., "A 36μW reconfigurable analog front-end IC for multimodal vital signs monitoring," *VLSIC*, pp. 170-171, Jun. 2017

[5] T. Zhou et al., "RMMIC: A 40μW Reconfigurable Multi-modal Multi-channel Interface Circuit System for Bio-signals Monitoring," *IEEE A-SSCC*, pp. 1-3, Nov. 2024.

[6] T. Seol et al., "A Hybrid Recording System with 10kHz-BW 630mV_{PP} 84.6dB-SNDR 173.3dB-FOM_{SNDR} and 5kHz-BW 114dB-DR for Simultaneous ExG and Biocurrent Acquisition," *ISSCC*, pp. 562-564, Feb. 2024.

[7] J. Koo, *et al,* "A Reconfigurable Multimodal Sensor Interface IC Based on Direct-Conversion ΔΣ Modulator Structure," *IEEE ISCAS*, pp. 1-5, May. 2024.

[8] Y. Li, *et al,* "A 15.5-ENOB 335 mVPP-Linear-Input-Range 4.7-GΩ-Input-Impedance CT-ΔΣM Analog Front-End With Embedded Low-Frequency Chopping," *IEEE SSC-L*, vol. 6, pp. 265-268, 2023.

[9] Q. Pan, *et al,* "A 0.5-mΩ/√Hz Dry-Electrode Bioimpedance Interface With Current Mismatch Cancellation and Input Impedance of 100 MΩ at 50 kHz," *IEEE JSSC*, vol. 58, no. 6, pp. 1735-1745, June 2023.